7-1-2015

# Hand use predicts the structure of representations in sensorimotor cortex.

Naveed Ejaz
*Institute of Cognitive Neuroscience, University College London, London, UK*

Masashi Hamada
*Department of Neurology, University of Tokyo, Tokyo, Japan*

Jörn Diedrichsen
*Institute of Cognitive Neuroscience, University College London, London, UK*

nature neuroscience

# Hand use predicts the structure of representations in sensorimotor cortex

Naveed Ejaz[1], Masashi Hamada[2] & Jörn Diedrichsen[1]

**Fine finger movements are controlled by the population activity of neurons in the hand area of primary motor cortex. Experiments using microstimulation and single-neuron electrophysiology suggest that this area represents coordinated multi-joint, rather than single-finger movements. However, the principle by which these representations are organized remains unclear. We analyzed activity patterns during individuated finger movements using functional magnetic resonance imaging (fMRI). Although the spatial layout of finger-specific activity patterns was variable across participants, the relative similarity between any pair of activity patterns was well preserved. This invariant organization was better explained by the correlation structure of everyday hand movements than by correlated muscle activity. This also generalized to an experiment using complex multi-finger movements. Finally, the organizational structure correlated with patterns of involuntary co-contracted finger movements for high-force presses. Together, our results suggest that hand use shapes the relative arrangement of finger-specific activity patterns in sensory-motor cortex.**



The production of skilled finger movements in humans relies on the activity of neurons in the hand area of primary motor cortex (M1)[1]. In contrast with the neighboring somatosensory cortex (S1), M1 lacks a strong somatotopic organization of finger representations[2,3]. We found that finger-specific patterns of activation, although stable in each individual, were highly variable across subjects. Does this apparent lack of organization reflect random variation or is there a common underlying principle that shapes the fine-grained patterns associated with each movement?

Previous results have suggested that neurons in M1 encode coordinated, rather than individual, finger movements. First, the areas in M1 that innervate each hand muscle are not segregated[4]. Second, neurons in M1 are not tuned to individual finger movements, but show broad tuning for movements of all five fingers and wrist[2,3]. Furthermore, activity patterns observed in fMRI for single finger movements are highly overlapping[5,6]. Finally, cortical stimulation of both humans[7,8] and monkeys[9] evokes simultaneous movements of multiple fingers, resembling the multi-joint movements observed during natural hand use.

We tested the hypothesis that the organization of cortical finger representations is determined by natural hand use. Given that hand usage patterns are relatively invariant across individuals[10], cortical finger representations should also be organized in an invariant fashion, even though they may show considerable spatial variability. We used fMRI and representational similarity analysis[11] to uncover this invariant organization and found that the fine-grained spatial activation patterns in M1 and S1 can be quantitatively predicted by the natural statistics of hand use.

## RESULTS

### Activity patterns for single-finger movements are variable across individuals

Using high-resolution functional imaging, we measured the activity patterns in six healthy participants during key presses of individual fingers of the right and left hands[12]. We analyzed the activity patterns for contralateral finger movements in the hand area of M1 and S1 for all available 12 hemispheres. **Figure 1** shows a surface representation of activity patterns in M1 for three individual subjects (see **Supplementary Fig. 1** for equivalent maps in S1). As reported earlier[5,6], there was no clear spatial segregation of finger activation patches. Instead, individual voxels were activated to varying degrees by all fingers, consistent with previous electrophysiological recordings that found that individual neurons have similarly broad tuning functions for finger movements[2,3].

The activity patterns were replicable and stable in each participant and hemisphere: split-half correlations of the patterns in participants were $r = 0.643$ (95% confidence interval, 0.558–0.715) for M1 and $r = 0.735$ (0.677–0.784) for S1. We also tested the long-term stability of digit representations in a different set of nine participants. Activity patterns were measured four times over a period of 6 months (Online Methods). If finger-specific patterns were perfectly stable, then the inter-session correlation should be as high as the within-session split-half correlations (**Fig. 2**). Even after 6 months, correlations were only 13.0 ± 5.3% for M1 and 14.6 ± 3.8% for S1 below the theoretical maximum.

In contrast to this within-subject stability, the size, shape and exact location of the activated areas varied considerably across individuals and hemispheres (**Fig. 1**). There was some consistency: when averaging activity patterns across participants (**Fig. 1**), a blurry somatotopic arrangement became visible with the thumb activating more ventral and the other fingers more dorsal areas of the motor strip. However, this organization only accounted for part of the replicable activity pattern; the correlation between the finger-specific activity patterns across all possible pairs of participants and hemispheres (Online Methods) was $r = 0.103$ (0.005–0.20) for M1 and $r = 0.235$ (0.148–0.317) for S1. This was the case, even though the inter-subject

[1]Institute of Cognitive Neuroscience, University College London, London, UK. [2]Department of Neurology, University of Tokyo, Tokyo, Japan. Correspondence should be addressed to J.D. (j.diedrichsen@ucl.ac.uk).

Received 31 March; accepted 7 May; published online 1 June 2015; doi:10.1038/nn.4038

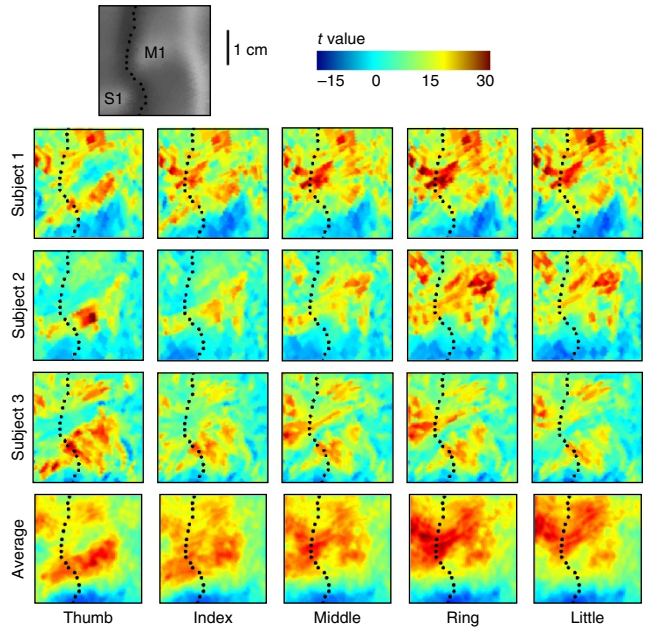


**Figure 1** Evoked activity patterns during single finger presses of the left hand in the hand area of the right primary motor cortex, recorded from three different participants at 3T. Results were normalized to a surface-based atlas. The dotted line indicates the fundus of the central sulcus. The upper inset shows the average sulcal depth. The last row shows the activity patterns averaged across all six participants. The hand knob[1] is located at the M1 label.

normalization led to a relatively precise alignment of the hand knob area of the primary motor cortex (**Supplementary Fig. 2a**). When we also drove the normalization by functional criteria (**Supplementary Fig. 2b** and Online Methods), the inter-subject correlations increased to $r = 0.244$ (0.180–0.307) for M1 and $r = 0.343$ (0.279–0.404) for S1. Thus, even with additional functional alignment, only 38% (M1; S1, 46%) of the reliable pattern variance across voxels could be accounted for by a systematic somatotopic arrangement shared across participants. The majority of the replicable pattern variance (M1, 62%; S1, 54%) was a result of a stable, but subject-specific, organization.

### Representational structure is invariant across subjects

We then asked whether these idiosyncratic patterns reflect random variation or whether their organization follows a common principle. Close inspection of **Figure 1** reveals some common features: for example, in all participants, the patterns for ring and little fingers were more similar to each other than to the thumb pattern. Thus, an invariant organization may be found in the relative similarities between activity patterns of each pair of fingers, rather than in their exact spatial distribution. We quantified these similarities using a cross-validated Mahalanobis distance (Online Methods)[13], which calculates the sum of squared voxel-by-voxel differences in activation, with each voxel weighted by the multivariate noise structure. A small pattern distance between two fingers implies that voxels that are activated for one finger are also activated for the other. Note that this measure considers the activation patterns as an unordered vector of voxel activities (**Fig. 3a**) and therefore disregards the location of voxels on the cortical sheet.

The distances between the ten possible pairs of fingers per hand were then arranged into a dissimilarity matrix (**Fig. 3b**)[11], which revealed a robust organization across individuals (see **Supplementary Fig. 3** for equivalent dissimilarity matrix for S1). The distances between the thumb and the remaining fingers were large, indicating a distinct activity pattern for this digit. In contrast, distances between middle and ring fingers were generally small, reflecting large overlaps of activity patterns. Across subjects and hemispheres (**Fig. 3c**), the relationship between these ten possible finger distances was well preserved. The average pairwise correlation, excluding the diagonal, was $r = 0.914$ (0.873–0.943) for M1 and $r = 0.924$ (0.892–0.947) for S1. This invariance was not solely a result of the thumb; the inter-subject correlation remained high even when the thumb was excluded (average pairwise correlation $r = 0.876$ (0.819–0.916) for M1 and $r = 0.904$ (0.841–0.943) for S1).

To what degree is this invariance caused by the blurred somatotopic arrangement visible in the average activity pattern (**Fig. 1**)? To test this, we removed the finger-specific mean pattern (calculated after functional alignment) from each individual map and recalculated the distances using only the subject-specific component. The resulting distance structure remained nearly unchanged and the inter-subject correlation remained high ($r = 0.894$ (0.834–0.933) for M1 and $r = 0.863$ (0.810–0.902) for S1), indicating that even the subject-specific patterns exhibited a common organization. This organization can be visualized in two dimensions using multidimensional scaling (**Fig. 3d** and Online Methods), reflecting the uniqueness of the thumb pattern, the orderly arrangement of the other fingers, and the fact that first digit is closer to the fifth than the third and fourth digits.

Together, these results reveal an invariant representational structure[11,14] for cortical finger representations. Specifically, the similarity between activation patterns for all possible finger pairs was highly preserved across individuals. This invariance was even present in the individual fine-grained patterns of activity and could not be explained by the common somatotopic arrangement of finger activation patches.

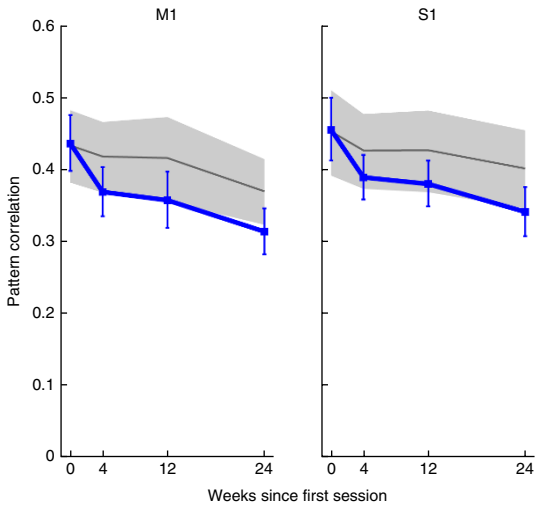


**Figure 2** Pattern stability across a period of 6 months in a group of nine separate participants. The correlation for week 0 is the split-half reliability of finger-specific patterns in the first testing session. Subsequent weeks show the average correlation between finger-specific patterns from the first session with patterns recording 4–24 weeks later. To make these values comparable to the split-half correlations, we based between-session correlations on half of the data from each session. The gray line indicates the theoretically attainable inter-session correlation if the patterns remained perfectly stable. Error bars (and shaded areas) indicate between-subjects s.e.m.

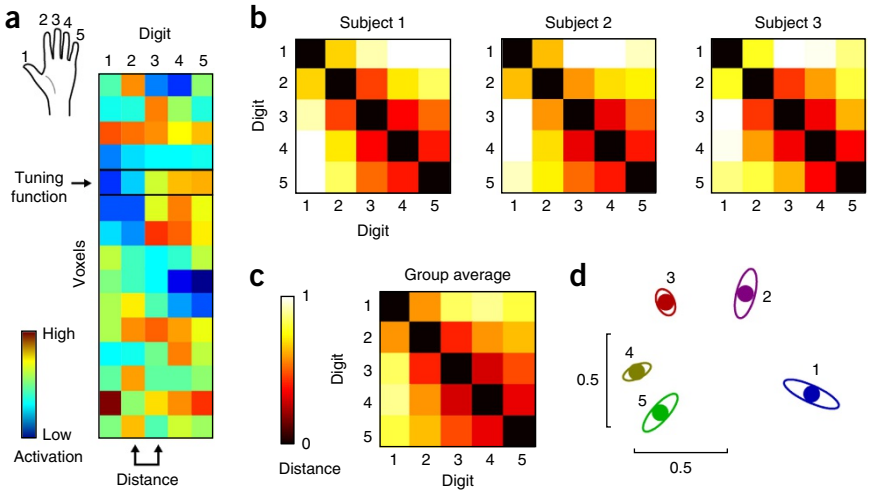


**Figure 3** Representational structure of finger movements in M1. (**a**) Activity patterns were concatenated into vectors of activations across voxels. Each row of the matrix constitutes the tuning function of a voxel over the five fingers, and each column represents the activity pattern for one of the fingers. (**b**) Cross-validated Mahalanobis distances between patterns for all digits in right M1 for the three participants depicted in **Figure 1**. (**c**) Distances between activity patterns averaged over the 12 hemispheres. (**d**) Multi-dimensional scaling of the pattern distances in two-dimensional space. Ellipses show s.e.m. after Procrustes alignment across participants corrected for the reduction in variability induced by the alignment. See **Supplementary Figure 3** for equivalent analysis for S1.

### Representational structure at a higher spatial resolution

To ensure that the measured representational structure is not an artifact of the spatial averaging induced by the relatively low spatial fMRI resolution (3T scanner, 2.3-mm isotropic), we replicated the experiment using a higher resolution in a separate group of seven subjects (7T scanner, 1.4 mm isotropic). As in the 3T experiment, the representational structure of finger movements was characterized by similar patterns for the ring and little finger movements, with the thumb patterns being clearly distinct (**Supplementary Fig. 4**). This representational structure was again stable across individuals ($r$ = 0.803 (0.753–0.843) for M1 and $r$ = 0.846 (0.797–0.884) for S1) and was highly correlated across the 3T and 7T experiments ($r$ = 0.964 for M1, $r$ = 0.950 for S1).

### Natural statistics of hand use predicts single-finger pattern distances

Thus far, we have shown that the relative similarities (or overlap) between activity maps associated with single finger movements is highly preserved across individuals, even though the maps themselves exhibit large inter-individual variability. This suggests that the development of individual maps is guided by some factor that ensures that they all arrive at the same representational structure, without dictating their exact spatial layout. What is this factor?

We considered the idea that the structure of activation patterns is determined by the way we use our hands in everyday life[15]. Our everyday activities and interactions with objects impose a strong correlation structure on our finger movements[16,17]. For example, the middle and the ring fingers often move together to facilitate grasping, whereas the thumb typically moves independently[10].

We predicted that frequently co-occurring finger movements would lead to strong associations between the cortical modules that encode them. When an individual finger is moved, activation would automatically spread to these associated circuits. Thus, the hand-usage model predicts that fingers that often move together would also be associated with similar activation patterns. It should be noted that the measured activation does not necessarily imply that associated muscle activity is evoked, given that the BOLD signal mainly reflects synaptic processes, rather than spiking of output neurons[18–20]. Furthermore, pyramidal tract neurons can show substantial increases in firing without measurable changes in muscle activity[21]. Indeed, although the middle and ring fingers were associated with overlapping patterns of cortical activity, participants were able to individuate the two fingers well, with minimal force produced by the neighboring finger (right hand, 0.031 ± 0.02 N; left hand, 0.076 ± 0.0257 N).

To quantify predictions for the hand-usage model, we used an existing data set[10] in which six participants went about their daily activities while movements around 19 finger joints of the right hand were measured for 2–4 h per subject. Given that our task mainly required flexion of the metacarpal (MCP) joints, only movements around these five joints (**Fig. 4a**) were considered. We then calculated the Euclidean distances (**Fig. 4b**) between the standardized absolute joint velocities for each pair of fingers, with small distances reflecting highly correlated movements.

The hand-usage model explained the observed pattern distances quite well (**Fig. 4c–f**), with correlations reaching $r$ = 0.897 (0.848–0.931) for S1 in the 7T data set. The maximum achievable correlation is bounded by the measurement noise on the distance structure of each individual; this noise ceiling can be estimated on the basis of the inter-subject reliability of the distance structures (**Fig. 4e**,**f** and Online Methods). Although the correlation was clearly below its theoretical maximum for the 3T data, it fell close to the estimated bounds for the 7T data. This is largely because the distance between thumb and index patterns (distance 1–2) was estimated to be larger using higher resolution imaging (**Fig. 4c**,**d**), suggesting that these neighboring activation patches were better resolved at 7T. Overall, the data suggests that the similarity structure of cortical activation patterns closely reflect the co-occurrence of movements made in everyday life.

### No differences between dominant and non-dominant hands

We found no differences in the representational structure between right (dominant) and left (non-dominant) hands (ANOVA on hand differences; M1, $F_{9,50}$ = 0.33, $P$ = 0.962; S1, $F_{9,50}$ = 0.39, $P$ = 0.936). This lack of a difference raises the question of whether everyday usage patterns differed between hands. To investigate this, we used an unpublished data set[22] in which kinematic data was recorded for both hands while eight healthy right-handed participants performed everyday tasks. Although the predicted distance structure for the right hand correlated highly ($r$ = 0.936) with the one derived from the older data set[10], there were no significant differences between the structure of distances for the dominant and non-dominant hands ($F_{9,70}$ = 1.71, $P$ = 0.105; **Supplementary Fig. 5b**,**c**). Thus, although the dominant hand generally showed more activity, the correlation structure between fingers was not appreciably different from the non-dominant hand.

### Alternative models for single-finger pattern distances

Even though the hand usage model predicted the single-finger pattern distances well, the fit needs to be evaluated against other

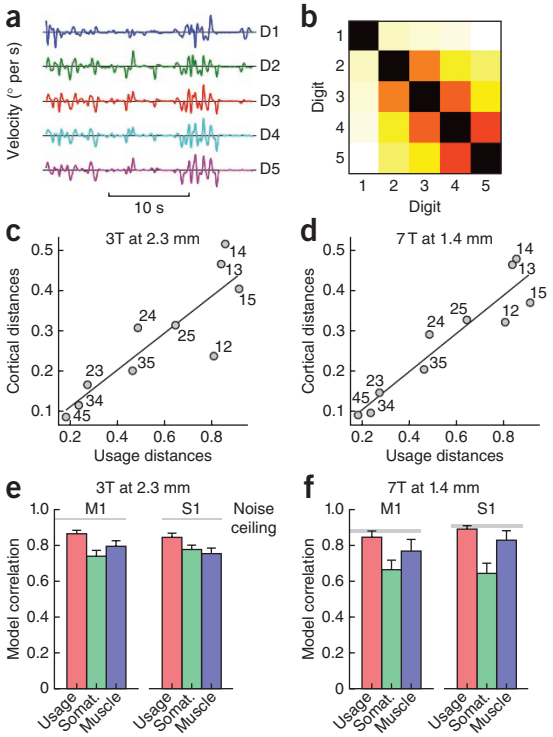


**Figure 4** Representational structure in M1 is best explained by natural statistics of hand use. (**a**) Raw velocities for a 30-s snippet of everyday movements around the MCP joints for each of the five digits. (**b**) The distance structure estimated by the MCP joint velocities. (**c**,**d**) Correlation between these predicted distances with the measured distances in M1 at 3T (2.3 mm, isotropic, **d**) and 7T (1.4 mm, isotropic, **d**). (**e**,**f**) Average correlation between predicted and measured inter-digit distances in M1 at 3T (**e**) and 7T (**f**). Error bars indicate s.e.m. and gray region indicates estimate of the best possible model fit (Online Methods).

competing models. We first considered how well an orderly somatotopic arrangement of digits along the cortical strip could explain the representational structure. For this model, finger activations patches were assumed to be overlapping Gaussian kernels sequentially arranged along the cortical strip (**Fig. 5a**). From these activation patterns, a predicted distance structure was calculated (**Fig. 5b**). The spatial width of the kernels (in arbitrary units with an inter-digit spacing of 1) was estimated to best fit the distance structure for each individual subject (1.55 ± 0.21 for M1 and 1.20 ± 0.41 for S1). The somatotopic model did not correlate with the cortical distances as well as the hand-usage model (**Fig. 4e**,**f**). Combined over the 3T (six participants × two hemispheres) and 7T (seven participants), this difference was significant for M1 (two-sided $t$ test, $t_{18} = 3.083$, $P = 0.006$) and for S1 ($t_{18} = 3.843$, $P = 0.001$).

Alternatively, we considered that the representational structure reflects the patterns of muscular activation associated with each movement, independent of natural use. The cortical activity patterns for the middle and ring fingers may have been similar because similar muscles are activated for movements of these two fingers. If M1 is assumed to represent hand muscles in an overlapping, yet independent, fashion (Online Methods), then the similarity of cortical activity patterns can be directly predicted from the similarity of the corresponding muscular activity patterns.

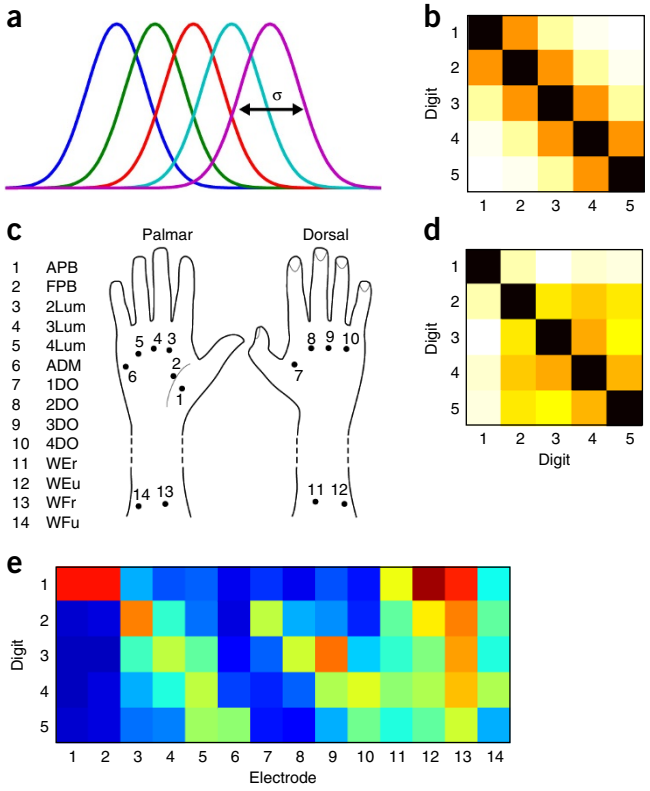


To test this idea, we recorded electromyogram (EMG) signals from 14 surface electrodes (**Fig. 5c**) while a separate set of seven subjects performed single-finger movements outside of the scanner. The distinct patterns of activity for each of the five individuated finger presses (**Fig. 5d**) were used to estimate the distance structure for the muscle model (**Fig. 5e**). Although this model correlated relatively well with the measured fMRI distances (**Fig. 4e**,**f**), the hand-usage model predicted the observed cortical activation pattern distances significantly better. This was the case for 15 of 19 measured hemispheres in M1 ($t_{18} = 3.236$, $P = 0.005$) and in 16 of 19 in S1 ($t_{18} = 3.642$, $P = 0.002$).

To summarize, our data suggest that the similarity structure of cortical activation patterns more closely reflects the co-occurrence of hand movements in everyday life than the similarity of muscle activations. The relatively good prediction by both models, however, also indicates that there is a tight correspondence between how we use our hands and the structure of muscle activity patterns necessary to generate these movements.

## Natural statistics predicts multi-finger distances

Although the agreement between natural movement statistics and the cortical activity patterns for single-finger movements is suggestive, real tasks typically require the coordinated movements of multiple

**Figure 5** Alternative models for explaining single-finger distances. (**a**) The somatotopic model assumes an orderly, and partly overlapping, arrangement of finger activation patches along the sensory-motor cortical sheet. The width of the Gaussian kernel was estimated from the empirical data. (**b**) Predicted distance structure for the somatotopic model. (**c**) 14 high-density electrodes were placed on the palmar and dorsal surface of the right hand, recording from abductor pollicis brevis (APB), flexor pollicis brevis (FPB), 2–4 lumbricales (Lum), abductor digiti minimi (ADM), 1–4 interossei dorsales (DO), and extensor (WE) and flexor (WF) muscles at the radial (r) and ulnar (u) sites of the forearm. (**d**) Predicted distance structure for the muscle model. (**e**) Average muscle activity, normalized by the peak activation across each channel, recorded from the 14 electrodes during the single finger task.

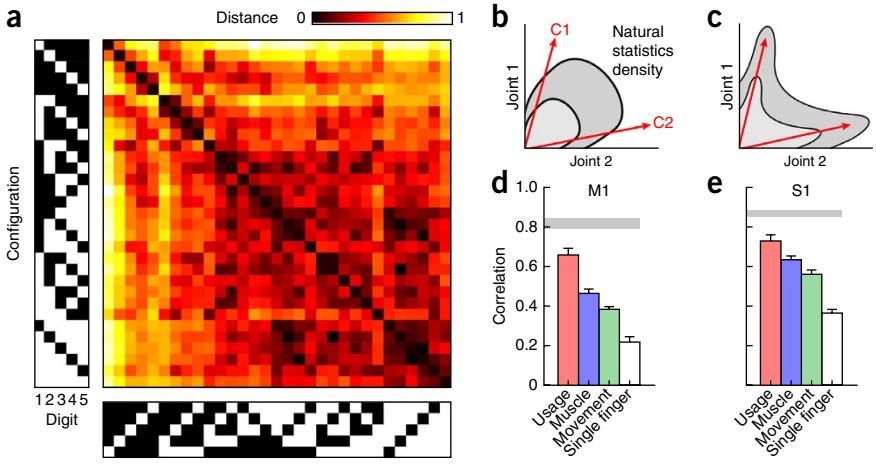


**Figure 6** Multi-finger configuration task. (**a**) The side panels show the tested 31 configurations, with white squares indicating that the corresponding finger had to exert a force of >2.6 N and black squares indicating that the finger had to stay relaxed on the keyboard. Middle, average pattern distances between the 31 configurations for primary motor cortex. (**b**,**c**) For the hand usage model, the distance between two configurations C1 and C2 will be small if they are similar to the same synergy (**b**), and large if they associated with different independent features of the underlying joint movement distribution (**c**). (**d**,**e**) Correlation between predicted and measured distances for the multi-finger configuration task in M1 and S1. Error bars indicate s.e.m. and gray region indicates the estimated range of the noise ceiling.

fingers[10]. The hand-usage model should therefore be able to predict the representational structure for complex multi-finger movements.

To test this idea, we asked eight participants to perform multi-finger presses with their right hand while we measured corresponding activity patterns using fMRI at 3T. Participants were trained to produce a series of finger configurations (**Fig. 6a**), each involving simultaneously pressing down with the instructed fingers while maintaining a baseline force with the others[23]. The entire set of 31 configurations resulted in a total of 465 pairwise distances. As with the single-finger task, the representational structure for the multi-finger task was notably stable across individuals, with an average inter-subject reliability of $r = 0.681$ (0.646-0.713) in M1 and $r = 0.765$ (0.735-0.792) in S1.

To evaluate whether this invariant representational structure could also be predicted by hand use, we averaged the angular velocities of the active fingers in the natural statistics data set. As for the single-finger task, we then determined the Euclidean distance between the standardized time series. If two different configurations were both similar to a frequently occurring joint-velocity combination, then their resultant distance would be small (**Fig. 6b**). If, however, each configuration was similar to independently occurring movements (**Fig. 6c**), then their distance would be large. As predicted, the hand-usage model correlated highly with the cortical distances ($r = 0.667$ (0.596–0.727) for M1 and $r = 0.738$ (0.683–0.784) for S1; **Fig. 6d**,**e**).

### Alternative models for multi-finger pattern distances

As with the single-finger experiment, we explored a range of competing models for explaining the multi-finger pattern distances (**Fig. 6d**,**e**). First, we considered the muscle model. EMG activity was recorded in a separate group of seven participants who performed the multi-finger task and the distances between all possible pairs of 31 muscle activation patterns were calculated. The correlations of the muscle model with the cortical distances were lower than those for the hand-usage model for all eight subjects, with the difference being highly significant ($t_7 = 7.015$, $P = 0.0002.1$ in M1 and $t_7 = 4.227$, $P = 0.0039$ in S1). This result cannot be explained by differences in reliability of the measures underlying each model (Online Methods).

We then considered the possibility that the predictions of the hand-usage model are simply a result of the physical similarity of joint movements for two configurations (the distance between C1 and C2; **Fig. 5b**,**c**) rather than the probability density of natural movements. We therefore correlated the cortical distances with the Euclidian distance between the normalized movement vectors for each configuration, without taking the natural statistics data in account. The correlations were lower than for the hand-usage model (**Fig. 6d**,**e**), indicating that the statistics of natural movement rather than the physical similarity of the configurations are critical for the model's goodness of fit.

We also investigated whether the representation of finger movements is shaped by a combination of both hand usage and muscle activity. Cross-validation was used to prevent over-fitting in this combined model, with the mixture proportion for the two models estimated on seven participants and the fit evaluated on the eighth. Including muscle activity distances into the predictions of the hand-usage model did not significantly improve the fit in M1 ($t_7 = 1.405$, $P = 0.203$), but did lead to significant improvements in S1 ($t_7 = 4.787$, $P = 0.002$).

Finally, we determined whether the observed distance structure for multi-finger movements could be predicted by a linear combination of the single-finger representations. When the measured distances from the single-finger task were used to predict the structure in the multi-finger experiment, low correlations were obtained (**Fig. 6d**,**e**), indicating that nonlinear interactions between different fingers need to be taken into account. In sum, these results strongly suggest that hand usage, rather than anatomical constraints, shape the reliable cortical representations for both simple and complex finger movements.

### Pattern distances correlates with structure of finger enslaving

What are the behavioral consequences of this representation? We hypothesized that, through intra-cortical connections, activity

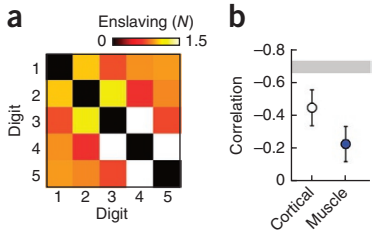


**Figure 7** Enslaving during single finger movements. (**a**) Averaged co-contraction (r.m.s. relative to baseline) in the un-instructed fingers when seven participants produced a 75% of maximal force with the instructed finger. The matrix was symmetrized. The average inter-subject reliability of the enslaving pattern was $r = 0.620$ (0.457–0.742). (**b**) Spearman rank correlation between the structure of force enslaving and the hand-usage and muscle models. Error bars indicate s.e.m. and gray region indicates estimates of the upper and lower bounds of the best possible model fit.

associated with an isolated finger movement spreads to circuits associated with normally co-occurring movements. As pointed out above, this overflow did not lead to substantial force production in the uninstructed fingers for the low force levels required during imaging. However, during near-maximal or maximal voluntary contractions (MVCs), neighboring fingers often show co-contraction, or 'enslaving'[24]. We therefore predicted that enslaving would be stronger for finger pairs with similar activity patterns and weaker for pairs with distinct patterns.

To test this idea, we asked seven participants to perform individuated finger presses at 75% of MVC (Online Methods). The result (**Fig. 7a**) shows the well-known co-contraction of neighboring fingers[24]. Enslaving was also found between the thumb and little finger, reminiscent of the smaller distance between thumb and little finger pattern in the cortical representation. Indeed, the enslaving structure correlated more negatively (that is, better, as small distances predict stronger enslaving; **Fig. 7b**) with the cortical than with the muscular distances ($t_6 = 4.903$, $P = 0.003$). This result is consistent with the notion that enslaving has, in part, a cortical origin[25–27].

## DISCUSSION

Our results uncover an invariant representational structure for simple and complex hand movements in M1 and S1. The relative similarities between activity patterns[11,14] were preserved across individuals, despite the substantial spatial inter-subject variability of the activity patterns themselves. The representational structure remained invariant even when the shared somatotopic arrangement of the digits was removed from the data. This suggests an organizing mechanism that shapes the overlap between patterns without enforcing a regular spatial layout.

The representational structure could be predicted by the natural statistics of hand use. Especially for complex multi-finger movements, the usage model outperformed a muscle model, which tested the idea that two cortical activity patterns are similar simply because the associated movements require similar muscles. This model assumes that the activity patterns associated with each muscle movement are uncorrelated in M1, ignoring the natural statistics of muscle activity. Thus, the inferior fit of the muscle model does not necessarily indicate that M1 represents movements rather than muscles[28], but that such muscle representations must be highly structured. Indeed, our results are compatible with the idea that representations of single muscles are predictable from the correlations between muscle activities during everyday movements[9]. However, because humans cannot voluntarily activate individual hand muscles, we needed to base our predictions on correlations between individual finger movements rather than between individual muscles activations.

Two studies have shown that the movements elicited by cortical stimulation resemble the main elements of everyday action[7,9]. However, the fact that M1 output reflects the structure of natural hand use does not necessarily imply that fMRI activity patterns should do so as well, as these mostly reflect excitatory synaptic activity[20]. On the contrary, if the cortex had simply evolved to optimally activate neural synergies that are encoded in the spinal cord, then M1 would have to produce two very different activity patterns to individuate two fingers that normally move together[29]. We found that the correlation structure of everyday hand use also dictates the similarity structure of cortical activity patterns. The overlap of these patterns is most likely determined by the strength of intra-cortical connections within M1. The spread of activation along these connections could also explain the patterns of muscle activity elicited by cortical stimulation[9,30], as well as the pattern of finger-enslaving at high force levels.

As a result of the inherently limited spatial resolution, the similarity between fMRI patterns can only measure the similarity of the underlying neural population activities if functionally similar circuits are sufficiently clustered. The higher spatial resolution at 7T allowed us to resolve thumb and index finger representations better and improved the fit of the hand-usage model. Nonetheless, many important aspects of the spatial activity structure may remain invisible to fMRI investigations.

A second limitation of our study was that the hand-usage model was based only on movement kinematics and did not take into account contact forces or sensory input. However, the similar representational structures in M1 and S1 raise the possibility that the observed patterns reflect, to a large degree, how sensory information from the skin, muscles and tendons is represented on the cortical sheet. Because sensory input it most often caused by movement, it is likely that the statistical structure of sensory input is tightly related to that of movement. Furthermore, sensory information from each part of the hand projects to the circuits involved in making the associated movements[31,32]. In fact, we observed high correlations in activity patterns between movements and sensory stimulation[5]. This tight correspondence makes it difficult to experimentally dissociate sensation and movement.

Overall, our data provide a quantitative evaluation of the idea that hand usage shape cortical representations[15] and is consistent with the idea that the invariant representational structure is the result of an unsupervised learning process that arranges finger representations on a two-dimensional cortical sheet. Through this learning process, movements that frequently occur together are mapped together following a 'like attracts like' principle[33]. For example, under a generalized Hebbian learning rule, the synaptic weights of a cortical network would represent the principal components of the natural statistics data[34]. The resulting activity patterns associated with independent finger movements should therefore exhibit a correlational structure that matches that of the correlations occurring during everyday use. Given that the statistics of natural hand movements are very similar across individuals[10], this learning rule will tightly determine the relationships between activity patches for different movements.

In contrast, the spatial arrangement of maps resulting from such a learning process can be much more variable[15]. This is because many different spatial arrangements satisfy the same representational structure, and the choice between these possible solutions will be determined only by slight differences in initial conditions. Thus, invariances in the spatial arrangement, such as the consistent ventral-dorsal somatotopic organization of the digits must be determined by alternative mechanisms, such as molecular gradients during development[35,36].

Our results suggest that the intrinsic connectivity of motor cortex is shaped the probability distribution of its activation states[37]. Quantifying this invariant representational structure constitutes a crucial first step toward understanding cortical changes associated with learning, aging or disease.

## METHODS

Methods and any associated references are available in the online version of the paper.

*Note: Any Supplementary Information and Source Data files are available in the online version of the paper.*

### ACKNOWLEDGMENTS

We thank J. Ingram and D. Wolpert, as well as A. Faisal and A. Thomik, for sharing their natural statistics data sets, G. Prichard, S. Clare, J. O'Reilly for help with the acquisition of the 7T data set, and J. Xu, B. Hertler, M. Brentscheidt, M. Wilmer,

A. Luft, P. Celnik and J. Krakauer for sharing the data regarding stability of finger representations. Finally we thank J. Krakauer, J. Xu, K. Longden and A. Saleem for helpful comments on the manuscript. The research was supported by grants by the Wellcome trust (094874/Z/10/Z) and James McDonnell foundation to J.D. The Wellcome Trust Centre for Neuroimaging is supported by core funding from the Wellcome Trust (091593/Z/10/Z).

## AUTHOR CONTRIBUTIONS

N.E. and J.D. were jointly responsible for design of experiments, analysis and writing of the manuscript. N.E. contributed the data for the multi-finger experiment and M.H. was instrumental in the muscle activity recording.

## COMPETING FINANCIAL INTERESTS

The authors declare no competing financial interests.



1. Yousry, T.A. *et al*. Localization of the motor hand area to a knob on the precentral gyrus. A new landmark. *Brain* **120**, 141–157 (1997).
2. Schieber, M.H. & Hibbard, L.S. How somatotopic is the motor cortex hand area? *Science* **261**, 489–492 (1993).
3. Schieber, M.H. Motor cortex and the distributed anatomy of finger movements. *Adv. Exp. Med. Biol.* **508**, 411–416 (2002).
4. Rathelot, J.A. & Strick, P.L. Muscle representation in the macaque motor cortex: an anatomical perspective. *Proc. Natl. Acad. Sci. USA* **103**, 8257–8262 (2006).
5. Wiestler, T., McGonigle, D.J. & Diedrichsen, J. Integration of sensory and motor representations of single fingers in the human cerebellum. *J. Neurophysiol.* **105**, 3042–3053 (2011).
6. Indovina, I. & Sanes, J.N. On somatotopic representation centers for finger movements in human primary motor cortex and supplementary motor area. *Neuroimage* **13**, 1027–1034 (2001).
7. Gentner, R. & Classen, J. Modular organization of finger movements by the human central nervous system. *Neuron* **52**, 731–742 (2006).
8. Gentner, R. *et al*. Encoding of motor skill in the corticomuscular system of musicians. *Curr. Biol.* **20**, 1869–1874 (2010).
9. Overduin, S.A., d'Avella, A., Carmena, J.M. & Bizzi, E. Microstimulation activates a handful of muscle synergies. *Neuron* **76**, 1071–1077 (2012).
10. Ingram, J.N., Kording, K.P., Howard, I.S. & Wolpert, D.M. The statistics of natural hand movements. *Exp. Brain Res.* **188**, 223–236 (2008).
11. Kriegeskorte, N., Mur, M. & Bandettini, P. Representational similarity analysis - connecting the branches of systems neuroscience. *Front. Syst. Neurosci.* **2**, 4 (2008).
12. Diedrichsen, J., Wiestler, T. & Krakauer, J.W. Two distinct ipsilateral cortical representations for individuated finger movements. *Cereb. Cortex* **23**, 1362–1377 (2013).
13. Nili, H. *et al*. A toolbox for representational similarity analysis. *PLoS Comput. Biol.* **10**, e1003553 (2014).
14. Haxby, J.V., Connolly, A.C. & Guntupalli, J.S. Decoding neural representational spaces using multivariate pattern analysis. *Annu. Rev. Neurosci.* **37**, 435–456 (2014).
15. Graziano, M.S. & Aflalo, T.N. Mapping behavioral repertoire onto the cortex. *Neuron* **56**, 239–251 (2007).
16. Santello, M., Flanders, M. & Soechting, J.F. Postural hand synergies for tool use. *J. Neurosci.* **18**, 10105–10115 (1998).
17. Santello, M., Flanders, M. & Soechting, J.F. Patterns of hand motion during grasping and the influence of sensory guidance. *J. Neurosci.* **22**, 1426–1435 (2002).
18. Logothetis, N.K., Pauls, J., Augath, M., Trinath, T. & Oeltermann, A. Neurophysiological investigation of the basis of the fMRI signal. *Nature* **412**, 150–157 (2001).
19. Attwell, D. & Iadecola, C. The neural basis of functional brain imaging signals. *Trends Neurosci.* **25**, 621–625 (2002).
20. Lauritzen, M. Reading vascular changes in brain imaging: is dendritic calcium the key? *Nat. Rev. Neurosci.* **6**, 77–85 (2005).
21. Kraskov, A. *et al*. Corticospinal mirror neurons. *Phil. Trans. R. Soc. Lond. B* **369**, 20130174 (2014).
22. Thomik, A.A.C., Fenske, S. & Faisal, A.A. Towards sparse coding of natural movements for neuroprosthetics and brain machine interfaces. *7th Int. IEEE/EMBS Conf. Neural Eng.* 938–941 (2015).
23. Waters-Metenier, S., Husain, M., Wiestler, T. & Diedrichsen, J. Bihemispheric transcranial direct current stimulation enhances effector-independent representations of motor synergy and sequence learning. *J. Neurosci.* **34**, 1037–1050 (2014).
24. Zatsiorsky, V.M., Li, Z.M. & Latash, M.L. Coordinated force production in multi-finger tasks: finger interaction and neural network modeling. *Biol. Cybern.* **79**, 139–150 (1998).
25. Zatsiorsky, V.M., Li, Z.M. & Latash, M.L. Enslaving effects in multi-finger force production. *Exp. Brain Res.* **131**, 187–195 (2000).
26. Lang, C.E. & Schieber, M.H. Human finger independence: limitations due to passive mechanical coupling versus active neuromuscular control. *J. Neurophysiol.* **92**, 2802–2810 (2004).
27. Yu, W.S., van Duinen, H. & Gandevia, S.C. Limits to the control of the human thumb and fingers in flexion and extension. *J. Neurophysiol.* **103**, 278–289 (2010).
28. Kakei, S., Hoffman, D.S. & Strick, P.L. Muscle and movement representations in the primary motor cortex. *Science* **285**, 2136–2139 (1999).
29. Mollazadeh, M., Aggarwal, V., Thakor, N.V. & Schieber, M.H. Principal components of hand kinematics and neurophysiological signals in motor cortex during reach to grasp movements. *J. Neurophysiol.* **112**, 1857–1870 (2014).
30. Diedrichsen, J. & Classen, J. Stimulating news about modular motor control. *Neuron* **76**, 1043–1045 (2012).
31. Rosén, I. & Asanuma, H. Peripheral afferent inputs to the forelimb area of the monkey motor cortex: input-output relations. *Exp. Brain Res.* **14**, 257–273 (1972).
32. Lemon, R.N. Variety of functional organization within the monkey motor cortex. *J. Physiol. (Lond.)* **311**, 521–540 (1981).
33. Durbin, R. & Mitchison, G. A dimension reduction framework for understanding cortical maps. *Nature* **343**, 644–647 (1990).
34. Sanger, T.D. Optimal unsupervised motor learning for dimensionality reduction of nonlinear control systems. *IEEE Trans. Neural Netw.* **5**, 965–973 (1994).
35. Donoghue, M.J. & Rakic, P. Molecular gradients and compartments in the embryonic primate cerebral cortex. *Cereb. Cortex* **9**, 586–600 (1999).
36. Gitton, Y., Cohen-Tannoudji, M. & Wassef, M. Specification of somatosensory area identity in cortical explants. *J. Neurosci.* **19**, 4889–4898 (1999).
37. Berkes, P., Orban, G., Lengyel, M. & Fiser, J. Spontaneous cortical activity reveals hallmarks of an optimal internal model of the environment. *Science* **331**, 83–87 (2011).

## ONLINE METHODS

All experimental procedures were approved by the research ethics committees at University College London, Johns Hopkins University, Columbia University and University of Zurich. No power calculation was used to pre-determine sample sizes but our sample sizes are similar to those reported in previous publications[12].

**fMRI single-finger experiment at 3T.** The empirical data are drawn from a published paper[12]. Six healthy right-handed participants (two females, four males, mean age = 25.9 years, s.d. = 5.1) performed individuated finger movements using both their left and right hands. Participants placed their fingers on a custom-built keyboard device with ten piano-like keys. Each key was equipped with a force transducer (Honeywell FS series) that measured the applied force with a repeatability of <0.02 N. Visual feedback was provided via a back projection screen.

Each trial started with the presentation of a keyboard outline with the target key highlighted in green for 1.36 s. The instruction was then removed and a go-cue signaled participants to make a short isometric force press with the instructed finger. The finger press needed to exceed 2.3 N, in which case the cue turned blue. After 1.36 s, the cue turned white again, signaling the next finger press. After five finger presses, the trial (total length of 8.16 s) ended.

During task performance, functional images were acquired using a 3T Siemens TRIO scanner with a 32-channel head coil. For each participant, eight runs were conducted, using a two-dimensional echo-planar imaging sequence (TR = 2.72 s, 32 slices, 126 volumes per run, slice thickness 2.15 mm, 0.15-mm gap, in-plane resolution 2.3 × 2.3 $mm^2$). Each run consisted of three repetitions of each of the ten fingers in random order, plus five randomly interspersed rest phases lasting 13.6–16.3s. A T1-weighted anatomical scan (3D MPRAGE sequence, 1-mm isotropic, 240 × 256 × 176 mm FOV) was also acquired.

**fMRI experiment to assess stability across sessions.** In a separate study, we established the stability of digit representations in M1 and S1. Nine healthy control participants were scanned four times over the course of a 6-month period, at weeks 0, 4, 12 and 24, performing the single finger task with their left and right hands. Functional scan were obtained on two different 3T Achieva Philips systems (Johns Hopkins University and University of Zürich). Otherwise, the protocol was identical to the one described above, although only four fingers (excluding the ring finger) were tested. All functional scans were aligned to the anatomical image obtained in the first testing session and re-sliced into the same voxel space.

**fMRI single-finger experiment at 7T.** Seven subjects (four females, three males, mean age = 25.6 years, s.d. = 2.6) were placed inside a Siemens 7T scanner (FMRIB). Functional images were acquired at a 1.4-mm isotropic resolution (TR = 3.0 s, 47 slices, 107 volumes per run). The design was identical to the one employed in the 3T study, although only the activity patterns associated with the five digits of the right hand were measured.

**fMRI multi-finger experiment at 3T.** The multi-finger experiment was similar in structure to the 3T single-finger experiment and consisted of eight healthy right-handed participants (four male, four female, mean age = 23.3 years, s.d. = 2.8). Participants were first trained to produce each of the 31 possible combinations of finger presses with the right hand over a period of 3 d (1.5 h $d^{-1}$). Following training, participants then performed the multi-finger task inside the scanner while functional imaging data was collected.

Following the presentation of the instruction cue, which showed the target finger highlighted in green (2 s), participants made three short isometric presses of the instructed finger configuration. Participants were required to maintain a baseline force of 0.6 N with the passive while reaching a force of 2.6 N on each of the instructed fingers. Each trial lasted 13.5 s and each of the 31 possible finger configurations was tested once per imaging run. Each participant was scanned over three sessions (1.5 h per session) for a total of 24 imaging runs.

**Imaging analysis.** Functional data was realigned for motion across runs and sessions, co-registered to the individual anatomical scan, and then analyzed with a generalized linear model using a separate regressor for each finger/configuration and run. The activation of each trial was modeled using a boxcar function (duration: 8 s for single-finger, 10.8 s for multi-finger task) and convolved with a standard hemodynamic response function. The regression parameter estimates and residuals from this analysis were then used to calculate the distance measures and pattern correlations (see below).

Anatomical T1 images were used to reconstruct the pial and white-gray matter surfaces using Freesurfer[38]. Surfaces were registered across participants and hemispheres using spherical alignment. Individual surfaces were morphed to match a template, first in terms of the sulcal depth map, and in a second step in terms of the local curvature, resulting in a nearly perfect overlap of the fundus of the central sulcus across participants[39] (**Supplementary Fig. 2a**).

The anatomical regions of interest (ROIs) were defined on the group surface using probabilistic cytoarchitectonic maps aligned to the average surface[40]. These regions were then projected into the individual brains via the reconstructed individual anatomical surfaces. This approach ensures a precise definition of ROIs, respecting the individual's folding anatomy. To analyze the hand representation in M1, all surface nodes with the highest probability for Brodmann area (BA 4) 2 cm above and below the hand knob[1] were selected. Similarly, the hand region in S1 was isolated using BA 3a, 3b, 1 and 2 (combined), again 2 cm above and below the hand knob. To avoid possible contamination of signals across the central sulcus, all voxels that had more than 25% of their volume located on the opposite side of the sulcus were excluded.

**Evaluation of activity patterns.** For the visual display of finger representations in M1 (**Fig. 1**) and S1 (**Supplementary Fig. 1**), *t* values (each finger > rest) were projected onto a flattened version of each individual surface. As in the ROI definition, a 25% exclusion criterion was used to avoid artificial mirroring of signals across the sulcus.

To evaluate the within-subject reliability of activation maps, we split the functional data into two halves (odd and even runs) and subtracted the mean activity pattern (averaged across fingers) from each half. The average correlation between patterns for the same finger across the two halves was then calculated.

To evaluate the consistency of activation maps across participants, we calculated the average correlation between all possible aligned functional maps of the same finger. To make the correlations comparable to the within-person correlations, each map was based on half the data and each pairing of halves was used. If the activity patterns are assumed to be composed of a pattern component that is shared across participants (α), a component that is systematic, but idiosyncratic to each participant (β), and a noise component (ε), then we can determine the amount of shared variance ($\sigma_\alpha^2$) as a proportion of the total explainable variance ($\sigma_\alpha^2 + \sigma_\beta^2$)[41] from the average within- and between-subject correlations. Under above assumption the within-subject correlation is $r = (\sigma_\alpha^2 + \sigma_\beta^2)/(\sigma_\alpha^2 + \sigma_\beta^2 + \sigma_\varepsilon^2)$, and the average between-subject correlation is $r = \sigma_\alpha^2/(\sigma_\alpha^2 + \sigma_\beta^2 + \sigma_\varepsilon^2)$.

For inter-subject alignment, we initially relied on anatomically driven normalization (see above), which superimposed the hand knob area well across participants (**Supplementary Fig. 2a**). We also judged the functional alignment, by mapping the average pattern distance (see distance measures), averaged over all 10 digit pairs, onto the flat-map (**Supplementary Fig. 2b**). Areas with large distance indicate regions in which movements of single fingers evoked significantly different activity patterns. To further improve the inter-subject alignment, we started from the solution found by anatomical normalization and then locally optimized (on 5 × 5-cm large sheet around the hand area) the correlation between functional distance maps of each participant/hemisphere and a group-averaged functional map. The shifts of the maps required for the improved functional alignment were on average 0.63 mm (s.d. = 0.67 mm) in each of the spatial directions. Even though these shifts were rather small, they led to some increases in the correlation between the finger-specific patterns across participants.

**Stability of finger representations.** The stability of the digit-specific activity patterns was also estimated by dividing the data from each session into odd and even runs. The mean activation pattern was then subtracted for each half separately. For each ROI, we then calculated the voxel-by-voxel correlation between patterns associated with the same finger, either between the two halves in a single session (within-session correlation) or between any of the halves of two different sessions (between-session correlation). If the activity patterns did not change at all, the correlation between session *i* and *j* should be as high as the within-session correlations for each session, or, more precisely, equal to the geometric mean of the split-half correlations for session *i* and *j*, $r_{i,j} = \sqrt{r_{i,i} r_{j,j}}$. This value therefore constitutes a reference value for absolutely stable activity patterns (**Fig. 2**).

**Distance measure.** The dissimilarity between the activation patterns was measured for each finger pair ($\mathbf{x}_i$, $\mathbf{x}_j$) within each hand using the cross-validated Mahalanobis distance[13]

$$d^2_{i,j} = (\mathbf{x}_i - \mathbf{x}_j)^T_A \sum_A^{-1/2} \sum_B^{-1/2} (\mathbf{x}_i - \mathbf{x}_j)_B \quad (1)$$

where $A$ and $B$ signify data from independent crossvalidation folds. Here we calculated the distances using each possible pair of imaging runs and then averaged the resulting distances. Crossvalidation has the advantage of ensuring that the expected value of $d$ is zero if two patterns are not statistically different from each other. Therefore, the average inter-digit distance can be taken as a functional criterion to detect regions that differentiate between the finger movements of a hand. The *PxP* noise covariance between voxels ($\Sigma$) was estimated from the first-level regression model of the original time series for each run separately and regularized to ensure invertibility[42].

Similar results were also obtained when using correlations between activity patterns as a distance measure, with large correlations corresponding to small distances. We used here Mahalanobis distances, as they take into account the multivariate noise structure and do not dependent on the activity baseline.

Inter-subject invariance of the distance structure was quantified by calculating the correlation of the ten distances (for each digit pair) across all possible pairs of participants. The calculation excluded the diagonal of the dissimilarity matrix.

To visualize the distances between all possible finger pairs, we used classical multidimensional scaling (MDS). MDS projects the $N$-dimensional dissimilarity matrix into a lower-dimensional space such that the distances between finger pairs are preserved as well as possible[43]. MDS was performed on data from individual participants, and the projections averaged after Procrustes alignment. Because Procrustes alignment does not only remove the arbitrary rotation induced by MDS, but also some of the true inter-subject differences, the standard error-ellipses in all MDS plots were inflated by 1.9, a factor estimated in Monte-Carlo studies using the structure and noise level found in this data set.

**Statistical analysis of correlations.** Correlations between activity patterns (across voxels) or correlations between distances (across finger pairs) were calculated for each participant/hemisphere separately. We Fisher Z-transformed these values and then calculated the mean and standard error. Assuming normality, we could then determine the lower and upper bounds of the 95% confidence interval. The mean and the bounds were transformed back into correlations and reported as such in the text. All statistical tests were performed on Fisher Z-transformed values.

**Estimating the noise ceiling for model fits.** Given that the cortical pattern distances were estimated in the presence of measurement noise, even a perfect model would not result in a correlation of 1 with the distance estimates from each subject. To estimate a noise ceiling for the fits, we calculated the average correlation of each individual distance structure with the group mean[13], where the group mean serves as a surrogate for the perfect model. Because the individual distance structure is also averaged into this group mean, this value slightly overestimates the true ceiling. As a lower bound, each individual distance structure was also correlated with the group mean in which this individual was removed.

**Natural movement statistics recording.** The statistics for naturalistic hand movements in humans were taken from two independent studies. All reported model fits were based on a first study[10], in which six healthy male subjects (ages 31–43) wore a cloth glove with imbedded motion sensors (CyberGlove, Virtual Technologies) while they pursued everyday activities. Hand movement statistics were collected for each participant across multiple sessions, on average for 2.8 h per participant. The sensors measured the angular positions across the 19 degrees of freedom of the hand continuously at 83 Hz. Because our finger presses were mostly generated using the MCP joints, only data from these five channels were used.

The second study[22] was used to assess differences of natural statistics across hands. Eight healthy right-handed participants performed everyday tasks within a bedroom, kitchen and office environment, while kinematic data was recorded simultaneously from both hands. As with the previous study, only data from the five channels corresponding to the MCP joints was used.

**Natural movement statistic model.** For the single finger-experiment, we used the velocity time series corresponding to the MCP joints of the five fingers. To account for differences in scaling, each vector was normalized to a length of 1. The predicted distances were the Euclidian distances between these normalized velocity vectors

$$d_{i,j} = (\mathbf{v}_i - \mathbf{v}_j)^T (\mathbf{v}_i - \mathbf{v}_j) \quad (2)$$

Because of the normalization, this distance will be small if $v_i$ and $v_j$ are highly correlated and large when they are uncorrelated. For the multi-finger experiment, MCP velocities were first averaged for all instructed fingers for each configuration, and then the distances between these 31 normalized time series were calculated as for the single-finger model.

**Somatotopic model.** For this model, we assumed that the finger activation patches were arranged linearly and equidistant along the cortical sheet and had the shape of a Gaussian kernel with the same width. The degree of overlap was estimated to best fit the pattern distances from each participant. We then calculated the Euclidean distance between the Gaussian finger activation patterns, as for the experimental data.

Instead of assuming an equidistant arrangement, we also attempted to estimate the centers of the kernels by determining the center-of-gravity for each finger on the two-dimensional surface from the actual data. The resulting correlations of this model with the real cortical pattern distances, however, were lower than for the equidistant arrangement.

**Muscle activity recording.** Seven healthy volunteers (different from the imaging participants, one male, six female, mean age = 23.1 years, s.d. = 3.8) performed the single- and multi-finger tasks with the right hand while EMG activity was recorded from 14 locations along the dorsal and palmar surfaces of the hand and the forearm (**Fig. 2a**). Similar to the imaging task, participants were required to produce isometric forces, with either individual or multiple fingers, at a level specified by 25% of MVC for each finger (average finger forces, 4.8 ± 1.0 N). Each trial consisted of a short announce phase (2–3 s) following which the subject had to press and maintain force on the instructed finger(s) for approximately 3–4 s. A total of 15 blocks were measured per participant, each block containing a single repetition per trial type (participant 6 had only ten blocks).

Muscle activity was recorded using 14 high-density Ag/AgCl electrodes in a belly-tendon montage while the participant performed the task. The signal from each electrode was sampled at 1,000 Hz, de-meaned, rectified and low-pass filtered (fourth order butterworth filter, $f_c$ = 40 Hz). Finally, the processed EMG signals were averaged across each trial over a 3.5-s time window starting from the time when the instructed finger(s) first moved.

**Muscle model.** As for the fMRI analysis, cross-validated Mahalanobis distances (equation (1)) were used to determine the similarity of movements in muscle space. This distance metric is robust against changes in the scaling of the raw EMG signals in each channel, and in how signals from different muscles mix in the measurement electrodes.

The only assumption that needs to be made is that the measured signals ($\mathbf{y}$, a 14x1 vector) reflect an arbitrary linear mixture of activity of a set of muscles or muscle groups ($\mathbf{x}$), $\mathbf{y} = \mathbf{A}\mathbf{x}$. If the trial-by-trial variability on $\mathbf{y}$ is assumed to be mostly caused by variability in the underlying muscle activity ($\mathbf{x}$), then the variance-covariance matrix of the sensor signals ($\mathbf{y}$) depends only on the variance-covariance matrix of the muscles ($\Sigma_x$) and the mixing matrix $\mathbf{A}$: $\Sigma_y = \mathbf{A}\Sigma_x\mathbf{A}^T$. Thus the squared Mahalanobis distance between two actions $i$ and $j$ in sensor-space ($\mathbf{y}$) is equal to the Mahalanobis distance between the two actions in muscle space

$$\begin{aligned} d^2 &= (\mathbf{y}_i - \mathbf{y}_j)^T \sum_y^{-1} (\mathbf{y}_i - \mathbf{y}_j) \\ &= (\mathbf{x}_i - \mathbf{x}_j)^T \mathbf{A}^T \left(\mathbf{A} \sum_x \mathbf{A}^T\right)^{-1} \mathbf{A}(\mathbf{x}_i - \mathbf{x}_j) \\ &= (\mathbf{x}_i - \mathbf{x}_j)^T \sum_y^{-1} (\mathbf{x}_i - \mathbf{x}_j) \end{aligned}$$




doi:10.1038/nn.4038

This holds for any arbitrary **A**, as long as it is invertible (that is, as long as we measure with as many electrodes as muscle groups of interest). The average inter-subject reliability of the distance measure for the multi-finger experiment was $r = 0.707$ (0.668–0.742), providing evidence that a reasonable degree of invariance was indeed achieved.

Production of individuated finger movements requires the co-activation of specific combinations of muscles. The muscle model tested whether the representational structure can be explained by the correlation structure of muscle activity alone, without assuming any special correlation structure that is imposed by usage. Because both EMG signals and fMRI signals are weighted by their reliability (implicit in the Mahalanobis distance), this model also assumes that a muscle or muscle group that is reliably activated during the task would also have a reliable cortical representation.

**Equating model predictions for reliability.** One concern in the comparison of hand usage and muscle and models is that their predictions are derived from measured and therefore potentially noisy data. The predicted distances based on the data from a single participant will consist of a variance component that is shared across participants ($\sigma_\alpha^2$), and one that is that is unique to that participant or due to noise ($\sigma_\varepsilon^2$). Because the EMG and hand kinematics are measured from a separate set of participants, only the shared component can correlate with the fMRI distances. The average inter-subject correlation of predicted distances provides us with an estimate of the proportion of the shared component relative to the total variance, with $r = \sigma_\alpha^2/(\sigma_\alpha^2 + \sigma_\varepsilon^2)$. This is a concern as the inter-subject reliability was $r = 0.681$ (0.646–0.713), for the muscle model and 0.972 (0.966–0.977) for the hand usage model.

To equate the proportion of systematic variance across hand-usage and muscle model, we compared the mean prediction averaged over all seven participants for the muscle model with the prediction based on the data from single subjects for the hand usage model. Given the independence of different participants, the reliability of the averaged muscle model can be estimated to be $r = 0.942$, roughly matching the reliability of a single subject for the natural statistics data.

Despite nearly equated reliability, the cortical distances correlated significantly better with prediction of the hand usage model (averaged over individual subjects from the natural statistics data set) than with the average prediction from the muscle model, both for M1, $t_7 = 7.015$, $P = 0.0002.1$, and for S1, $t_7 = 4.227$, $P = 0.0039$.

**Estimating finger independence during movement.** To estimate the degree of co-contraction of adjacent fingers, the participants of the muscle recording study performed the same task at 75% MVC. Averaged across fingers, participants produced forces of $14.5 \pm 2.9$ N. The r.m.s. force deviation for each uninstructed finger from the pre-trial baseline was calculated. These values were then arranged in an enslaving matrix that shows the involuntary force change across passive fingers for presses of the instructed finger. Given the symmetry of the hand-usage and muscle models, this matrix was symmetrized for model comparison purposes. Spearman-rank correlations were used for model evaluation, as a linear relationship could not be assumed.

A **Supplementary Methods Checklist** is available.


38. Dale, A.M., Fischl, B. & Sereno, M.I. Cortical surface–based analysis. I. Segmentation and surface reconstruction. *Neuroimage* **9**, 179–194 (1999).
39. Fischl, B., Sereno, M.I., Tootell, R.B. & Dale, A.M. High-resolution intersubject averaging and a coordinate system for the cortical surface. *Hum. Brain Mapp.* **8**, 272–284 (1999).
40. Fischl, B. *et al.* Cortical folding patterns and predicting cytoarchitecture. *Cereb. Cortex* **18**, 1973–1980 (2008).
41. Diedrichsen, J., Ridgway, G.R., Friston, K.J. & Wiestler, T. Comparing the similarity and spatial structure of neural representations: a pattern-component model. *Neuroimage* **55**, 1665–1678 (2011).
42. Ledoit, O. & Wolf, M. Improved estimation of the covariance matrix of stock returns with an application to portfolio selection. *J. Empir. Finance* **10**, 603–621 (2003).
43. Borg, I. & Groenen, P. *Modern Multidimensional Scaling: Theory and Applications* (Springer-Verlag, New York, 2005).